

GT2017-63279

TRANSIENT MODELING OF A SUPERCRITICAL CO₂ POWER CYCLE AND COMPARISON WITH
TEST DATA

Vamshi K. Avadhanula
Echogen Power Systems (DE), Inc.
Akron, Ohio, USA

Timothy J. Held
Echogen Power Systems (DE), Inc.
Akron, Ohio, USA

ABSTRACT

A transient model of a commercially-available 7.3MWe sCO₂ power cycle was developed using an implicit 1-D Navier Stokes solver. The power cycle underwent extensive factory testing, which validated the component and system performance, and the design and performance of the control system. The model structure simulates the as-tested configuration of the power cycle, with major components consisting of water-cooled heat rejection heat exchanger, turbine-driven compressor, recuperator, primary heat exchanger, power turbine, gearbox and generator. Subsystem models are developed to validate individual component (compressor, drive turbine, power turbine, heat exchangers etc.) model performance against design data. The component models are then assembled into the full system model. For the system transient simulation, the input parameters (or boundary conditions) are taken from the test data. More than eight hours of test data is used in the present transient simulation. The simulation results, including thermodynamic state points, component performance and system performance, are compared against the corresponding test data.

NOMENCLATURE

dh_s = Isentropic enthalpy change
 dP = Pressure rise
 C_v = Valve flow coefficient
 N = Speed
 p = Pressure
 T = Temperature
 w = Mass flow rate
 Z = Compressibility factor
 γ = Isentropic expansion coefficient
 η_s = Isentropic efficiency
 η_p = Pump isentropic efficiency
 Φ = Flow coefficient
 Ψ = Head rise coefficient

Subscripts

a = Actual

c = Corrected

INTRODUCTION

Supercritical carbon dioxide (sCO₂) power cycles promise several advantages over conventional steam Rankine cycles, including higher efficiency, lower capital and operating costs, and water-free operation [1–3]. In addition, the small physical size of the turbomachinery is expected to facilitate more rapid response to changes in boundary conditions (e.g., heat source input or load demand signals) than steam systems. Due to the smaller physical footprint of the sCO₂ power cycle (a 10MWe system can be truck-shippable), it can efficiently be coupled to numerous applications such as nuclear power, solar power, waste and exhaust heat recovery as well as bottoming cycles for fossil fuel power plants.

To establish the potential for improved operability, and to define the optimal operation and control methodologies for these systems, comprehensive physics-based transient models are required. Although some early modeling results have been published, actual system operating data has been limited to laboratory-scale devices. However, recent advances [4] have led to the design, fabrication and test of the first MW-scale sCO₂ power cycle, making new data sets available for the development and validation of this type of model.

TEST CONFIGURATION

The EPS100 is a nominally 7.3MWe net power sCO₂ power cycle designed for commercial operation, utilizing the exhaust heat of a 20-25MWe gas turbine as the heat source. The details

of the production cycle configuration and of an updated version capable of over 9MWe from the same heat source, are described in Reference [5]. In its production configuration, the EPS100 uses a constant-speed “power” turbine connected to a gearbox-driven synchronous generator for power generation, and a separate, variable-speed turbocompressor to provide high-pressure CO₂ to operate the cycle. Two recuperators recover residual enthalpy from the turbine exhausts by preheating the working fluid, in combination with a set of “primary” heat exchangers that transfer heat from the external source to the working fluid, which then drives the two turbines. The two turbines operate over the same pressure ratio, but the turbine connected to the compressor (the “drive” turbine) utilizes somewhat lower-temperature fluid. It is this combination of sequential heat addition and recuperation stages, as well as expansion of a fraction of the lower-temperature fluid, that allows for optimal coupling of the variable heat capacity working fluid with the nearly constant heat capacity exhaust heat source.

For factory testing purposes, the EPS100 was reconfigured in a “simple recuperated” configuration, with one of the recuperators used instead as the primary heat exchanger, with the facility steam supply serving as the heat source (Fig. 1). Both turbines were connected to the same temperature fluid, and a separate throttle valve (FCV41) was added to permit independent control of the power turbine. Note that due to the low temperature of the available steam, the turbine inlet temperatures were limited to approximately 265°C. This temperature was high enough to operate the drive turbine at full load conditions, but the power turbine, with a design inlet temperature of 485°C, was limited to approximately 4MW of shaft power.

Several interrelated control loops provide stable operation of the system, and respond to boundary condition and commanded changes to the system operating state. In production service, the synchronous generator will be connected to the local or utility electrical grid, which then provides speed stabilization for the power turbine. For the factory test, the power generated by the cycle was dissipated by resistive air-cooled load banks. Thus, power turbine speed control was provided by the control system, as described in a following section. The compressor bypass valve (PCV2) controls turbocompressor speed, which affects compressor flow rate and pressure rise. Power turbine speed is controlled by a combination of bypass (TCV3) and throttle (FCV41) valves, and load bank resistance, which was operated manually. Finally, an inventory control system transfers working fluid into and out of the primary flow loop to actively control compressor inlet pressure [6]. The turbocompressor uses hydrostatic CO₂-supported bearings, supplied by the compressor discharge. A small control valve (PCV11) is used to regulate the flow rate of CO₂ to these bearings.

The complex interrelationships between these control loops impact the operability and control of the overall power cycle. For instance, the compressor bypass loop affects the outlet pressure of the compressor, which directly affects the inlet pressure of both turbines (including the turbine driving the compressor).

Thus, a perturbation in turbocompressor speed propagates into both the power turbine speed control and the turbocompressor work balance (drive turbine work relative to compressor work). The latter effect can create an unstable feedback loop that is only stabilized through the action of the control system. Similarly, a perturbation in the power turbine load will cause the power turbine speed to deviate from its set point. The control system action is to modulate the power turbine throttle valve to maintain speed. This modulation affects the overall system flow characteristic, which affects the load on the compressor, and thus also the speed of the turbocompressor.

The complex interactions of these control loops can result in deviations from the intended operating point and tuning them properly is time-consuming. Normal control tuning methods require significant perturbations of the control inputs, and monitoring the response of the system. These perturbations can place the system at risk if the response is uncontrollable, or places the operating point in an unacceptable condition. For this reason, an accurate, physics-based model of the system can be an invaluable aid in designing, improving and tuning control algorithms.

MODEL CONFIGURATION

The model structure simulates the as-tested configuration of the EPS100 power cycle on the GT-SUITE [7] system simulation software platform. GT-SUITE is a 1D engineering system simulation software, with tools for analyzing mechanical, flow, thermal, electromagnetic and control systems. In flow simulations (of present work), GT-SUITE solves 1D Navier-Stokes equations along flow components and solution convergence is checked using pressure, continuity and energy residuals. The models are built based on GT-SUITE supplied and/or user-defined component templates. Component templates can take manufacturer data and/or test data to calibrate the component. Individual components can then be simulated and validated using subsystem boundary conditions before being incorporated into full system model. These component templates are connected by piping components to build the full system model. GT-SUITE uses NIST REFPROP [8] for calculating fluid thermal and transport properties.

Figure 2 shows the sCO₂ power cycle model configuration with heat rejection heat exchanger, turbocompressor, recuperator, target heat addition, power turbine, gearbox and generator. Individual component models were first constructed and validated against the test data before they were assembled into the full system model. This process is explained in detail with recuperator example below and applies to many of the other components as well.

The major difference between test configuration of Fig.1 and model configuration of Fig. 2 are, (i) the recuperator and water-cooled heat rejection heat exchanger were both printed circuit heat exchanger (PCHE) [9] during testing, but were simulated as a plate heat exchanger (PHE), (ii) A piston accumulator is included at a fluid branch at the compressor inlet in the model,

to simulate an active inventory control system (ICS), (iii) the model does not yet incorporate the power turbine bypass valve (TCV3). This simplified approach for PCHE and ICS in modeling should not have any major impact on system dynamics in achieving the goals of this paper. The absence of TCV3 limits the range of conditions that can be modeled to those where TCV3 is closed (or nearly closed).

Heat Exchanger Models

Figure 3 shows the individual recuperator model in isolation. The recuperator is a PCHE, but is simulated as a PHE, with an increased heat transfer area multiplier to account for the high effectiveness of the PCHE geometry. The recuperator is a PCHE, but for convenience, is simulated using the built-in PHE model in GT-SUITE. From a heat transfer and pressure loss perspective, PCHEs and PHEs have very similar governing equations, as both are primarily counterflow geometry, and the fluid flow is well within the turbulent regime. Thus, the PCHE can be simulated by applying an increased heat transfer area multiplier to account for the smaller passage dimensions relative to a conventional PHE. The heat transfer process is discretized into 25 subvolumes to account for the variation in fluid properties as the temperature and pressure vary across the length of the heat exchanger. The thermal mass of the heat exchanger is set equal to the physical mass of the actual heat exchanger multiplied by the average heat capacity of the 316L stainless steel material.

The heat transfer process is modeled as a series of thermal resistances. The baseline heat transfer coefficients are modeled after classical Dittus-Boelter correlations with variable coefficients, with a simple one-dimensional thermal conduction resistance between the two fluids. The recuperator model is calibrated using a subset of steady-state data points taken from test data. The calibration process utilizes measured fluid flow rates, inlet temperatures, inlet and outlet pressures, and overall heat transfer rate. Using this information, the software adjusts the heat transfer and pressure drop coefficients to best match the supplied data.

The PCHE water-cooled heat rejection heat exchanger (HRHX) model is constructed and validated in a similar manner as the recuperator. As the EPS100 was designed to operate in both supercritical and transcritical (condensing) mode, the HRHX is modeled as a two-phase heat exchanger on the CO₂ side. For single-phase heat transfer, Dittus-Boelter correlations are used, while the correlation of Yan *et al.* [10] was used for condensation heat transfer.

The calibration process was validated by using a subcomponent model, which includes the heat exchanger and inlet conditions. The modeled outlet conditions are shown in Fig. 4 as a function of the measured outlet conditions. As can be seen, the agreement is excellent, with calculated weighted regression errors of 0.51% and 0.27% for overall heat transfer rate for the recuperator and HRHX respectively.

Due to the complexities of the steam condensation process and controls, and the fact that the steam-to-CO₂ heat exchanger

is not part of the production configuration, a detailed heat exchanger model was not used for this component. Instead, a targeted temperature was imposed on the CO₂ flow at the heat exchanger outlet as a boundary condition. For modeling purposes, this temperature was taken from the measured data.

Turbomachinery: Turbines and Compressor Models

Turbomachinery maps were used to model compressor, drive turbine and power turbine. Turbomachinery aerodynamic performance is modeled using two-dimensional maps, which are derived from mean line flow analysis of the components over a wide range of design point and off-design conditions. The transient simulation uses these maps to predict the flow rate and efficiency of the turbine through the following relationships:

$$w_c = f_w(N_c, dh_{sc}) \quad (1)$$

$$\eta_s = f_\eta(N_c, dh_{sc}) \quad (2)$$

$$N_c = f_N(N, \gamma, Z, T) \quad (3)$$

$$dh_{sc} = f_{dh}(dh_{sa}, \gamma, Z, p) \quad (4)$$

$$w_c = f_2(w, \gamma, Z, T, p) \quad (5)$$

Turbine maps are provided as two-dimensional tables for corrected mass flow rate and isentropic efficiency in terms of corrected speed and enthalpy change. An example representation of a turbine map is shown in Fig. 5. The maps are implemented as two-dimensional tables within the model, which are then linearly interpolated for the current operating conditions at each step.

The mechanical model of the turbomachinery, gearbox and generator uses the classical rotational inertia formulation to create the angular momentum conservation equation for the transient simulation. Mechanical losses are modeled from manufacturers' data for the turbine bearings, gearbox and generator. The bearing and gearbox losses are functions of power turbine speed, and generator loss is function of power turbine speed and power turbine load.

Compressor performance maps are derived in a similar manner as the turbine maps, using mean-line code calculations to calculate head rise and efficiency. The maps are two-dimensional tables, with flow coefficient and inlet fluid temperature as the primary correlating variables.

$$\eta_p = f_{\eta_p}(\Phi, T) \quad (6)$$

$$\Psi = f_{\Psi}(\Phi, T) \quad (7)$$

The dependence of flow and pressure rise on speed is incorporated into the definition of the above coefficients. The simulation uses linear interpolation to calculate the efficiency and head rise coefficients at each time step.

Valves and Control System Models

The control valves are simulated as variable-area orifices. For comparison purposes, the valve position is converted to an equivalent area based on the manufacturer-supplied curves of C_v as a function of percentage open. The valve positions are determined by the actions of the control system, as described below.

The simulation control loops are designed to replicate the control system as implemented in the test configuration, with the basic loop architecture as described previously and shown in Fig. 2. The control loops follow a basic proportional-integral configuration, with a measured parameter used as the feedback variable to drive the behavior of a control variable. An example is shown in Fig. 6, which depicts the power turbine speed control loop. The measured turbine speed is compared to an operator-supplied speed setpoint. The difference between the measured and setpoint speed is used to modify the throttle valve position, using classical proportional-integral (PI) formulations, with the proportional gain and integral times defined by the operator. Much of the process of “tuning” a control system consists of modifying these parameters to obtain optimal response time of the system to disturbances while maintaining fully stable operation.

For the purposes of the model control system tuning, an isolated power train loop with power turbine throttle valve is simulated with the inlet temperature and pressure, and outlet pressure supplied as boundary conditions. A submodel simulation is conducted, where the throttle valve position was changed in stepwise manner and the power turbine speed response was noted. Using this information, assuming first order linear behavior of the valve, the optimal proportional and integral gains for the control loop were determined. A similar method was adopted for compressor bypass valve control loop PI gains.

Compressor inlet pressure is controlled by inventory management. In lieu of a full model that includes the inner workings of the inventory control system (ICS), a simplified approach is taken. A piston accumulator is included at a fluid branch at the compressor inlet. The accumulator pressure is set to the measured compressor inlet pressure. To maintain the system pressure at the measured value, fluid is injected or withdrawn from the main fluid loop via the connection to the piston accumulator. The details of the control algorithm are not included in the model, but the appropriate physical behavior is replicated. Future versions of the model will include a more complete description of the ICS and control algorithms.

In summary, for the full system model, the boundary conditions are cooling water supply temperature and flow rate, primary heat exchanger CO₂ outlet temperature, and generator load. In addition, control parameter setpoints (turbocompressor speed, power turbine speed and compressor inlet pressure) are supplied as inputs to the transient model. For the system transient simulation, these input parameters are taken from the test data. The simulation results, including thermodynamic state points, component performance and system performance, are compared against the corresponding test data.

TRANSIENT SIMULATION RESULTS

The transient simulations are based on data collected during an extensive series of factory tests to evaluate operation, controls and performance [4]. Each day, the test system was run from a cold start to full load operation, with the goal of maximizing the

power turbine output. For these simulations, the boundary condition values (heat source and heat sink temperatures and flows) and control setpoints (turbocompressor speed, electrical power load and compressor inlet pressure) are taken from the test data, and input to the model. Since the model does not yet incorporate the power turbine bypass valve (TCV3), the initial state of the model is taken to be the condition where the bypass valve has fully (or nearly) closed, and the power turbine is partially loaded. The simulation begins by holding the initial boundary condition values constant for 2000 seconds of simulation time, which allows the model to reach a quasi-steady-state solution prior to allowing the boundary conditions to vary per the operating conditions of the test data set. Note that the system is not at a true quasi-equilibrium condition at this point, which may be responsible for some of the initial deviation between model and data.

The transient simulation is carried out for more than eight hours of simulation time, consistent with the test data set. Over the course of the simulation, the boundary conditions vary significantly. The cooling water flow rate varies from 260–300kg/s, supply temperature from 12.7–21.0°C. Primary heat exchanger CO₂ outlet temperature range was 263–270°C and generator load varied between 1100–3100kW.

After the initial simulation (“Simulation 1”) was completed, it was apparent that the model’s capability to maintain turbocompressor speed at the setpoint value was considerably better than the tuning parameters used in the test system (Fig. 7). This difference between simulation and test data is likely due to differences between the details of the control system software and non-ideal behavior of the sensors and actuators (valves), which are not yet fully simulated. Thus, an intermediate approach was taken initially. Rather than use the operator setpoint for the turbocompressor speed control, the measured value of speed was used as the control system setpoint in a second simulation (“Simulation 2”)—note that the simulation control system is still active in this procedure, but is tracking the measured speed by modulating the compressor bypass valve. The difference in bypass valve position between the two simulations is very small (Fig. 8), which illustrates how sensitive the turbocompressor speed is to this control parameter. The results of the two simulations are shown in Figs. 7–10. Once the turbocompressor speed is more accurately reproduced, the other parameters, particularly compressor outlet pressure (Fig. 9) and power turbine throttle valve position (Fig. 10), follow the test data much more closely. For the remainder of the comparisons, Simulation 2 is exclusively plotted against the data.

Heat exchanger performance is shown in Figs. 11–15. One area of particular interest is the performance of the HRHX as it transitions from subcritical, to transcritical, to fully supercritical behavior. In the early stages of the test (while the cooling tower water was at its lowest temperature), the HRHX inlet and outlet pressures are both below the critical pressure (see Fig. 9, as the HRHX outlet pressure is approximately the same as the compressor inlet pressure. From Fig. 12, the HRHX inlet pressure is approximately 0.3–0.4 MPa higher than the inlet pressure). The

HRHX inlet pressure transitions from subcritical to supercritical conditions at approximately 5000 seconds, while the HRHX outlet pressure increases to a supercritical condition around 9500 seconds. Following 9500 seconds, the entire heat rejection process occurs at supercritical pressure. It is interesting to note that the system behavior during this transition across the critical pressure line is well reproduced by the simulation, with no dramatic changes in overall or component-level performance.

Also, at around 16000 seconds, a sudden change in HRHX heat flux (Fig. 15) occurred due to the step change in water flow rate (Fig. 14) that resulted from manual operation of a water supply. The effect of this transient behavior was well captured by simulation which can also be observed by the rapid change in water outlet temperature in Fig. 13.

The simulations in general follow the test data closely after the initial transient period. In a notable exception to this agreement, the model under-predicts the heat flux through the recuperator by a considerable amount, while the pressure drop, and inlet and outlet temperatures are well-predicted on absolute basis (Figs. 11–12). The deviation in heat flux in recuperator is due to mismatch of recuperator flow rates from test data and simulation. This difference results from an unintentional 2.5 kg/s flow rate through the power turbine bypass valve (TCV3), which was caused by an improperly calibrated actuator. As TCV3 is not yet included in the model, this flow could not be accounted in the present modeling study (Fig. 14). The effect of not including turbine bypass valve in system simulation can also be observed in Fig. 8, where the flow through the turbine bypass valve is being accounted through an increased compressor bypass valve flow.

Turbomachinery performance is shown in Figs. 16–19. The predicted power output levels, flow rates and efficiency values are well-predicted by the model, indicating that the mean-line performance maps have good fidelity. Transient performance is more difficult to evaluate at present, as the selected data set does not contain any rapid changes in operating conditions. Once the turbine bypass valve (TCV3) has been incorporated into the model, further evaluations of transient model behavior, including startup, normal shutdown and emergency shutdown, will be conducted.

SUMMARY

A 7.3MWe capable sCO₂ power cycle was modeled and simulated in GT-SUITE system simulation software. Individual system components were modeled and validated before incorporating them into full system model. Transient simulation of full system model was carried out with boundary conditions supplied from test data. A simplified version of the control strategies from the test configuration were also incorporated into the model. Once the turbocompressor speed control setpoint was aligned with the measured test data, good agreement between transient

simulation results and test data was observed. The continuation of this work will include system modeling from startup to full load operation, which will require incorporation of different control strategies throughout the stages of startup.

REFERENCES

- [1] Persichilli, M., Held, T., Hostler, S., and Zdankiewicz, E., 2011, "Transforming Waste Heat to Power through Development of a CO₂ - Based Power Cycle," 16th Int. Symp. Compress. Users-Manufacturers, pp. 8–10.
- [2] Persichilli, M., Kacludis, A., Zdankiewicz, E., and Held, T., 2012, "Supercritical CO₂ Power Cycle Developments and Commercialization: Why sCO₂ can Displace Steam," Power-Gen India & Central Asia, pp. 1–15.
- [3] Held, T. J., Miller, J., and Buckmaster, D. J., 2016, "A Comparative Study of Heat Rejection Systems for sCO₂ Power Cycles," 5th Int. Supercrit. CO₂ Power Cycles Symp.
- [4] Held, T. J., 2014, "Initial Test Results of a Megawatt-Class Supercritical CO₂ Heat Engine," 4th Int. Symp. - Supercrit. CO₂ Power Cycles.
- [5] Held, T. J., 2015, "Supercritical CO₂ Cycles for Gas Turbine Combined Cycle Power Plants," Power Gen Int.
- [6] Close, C., 2016, "Mass Management System for a Supercritical Working Fluid Circuit." United States Patent Application # 20160010512.
- [7] Anonymous, 2016, "GT-SUITE Overview" [Online]. Available: <https://www.gtisoft.com/gt-suite/gt-suite-overview/>. [Accessed: 21-Nov-2016].
- [8] Lemmon, E.W., Huber, M.L., and McLinden, M.O., 2013, "NIST Standard Reference Database 23: Reference Fluid Thermodynamic and Transport Properties-REFPROP", Version 9.1, National Institute of Standards and Technology, Standard Reference Data Program, Gaithersburg.
- [9] Le Pierres, R., Southall, D., and Osborne, S., 2011, "Impact of Mechanical Design Issues on Printed Circuit Heat Exchangers," Proceedings of sCO₂ Power Cycle Symposium, Boulder, Colorado.
- [10] Yan, Y.-Y., Lio, H.-C., and Lin, T.-F., 1999, "Condensation heat transfer and pressure drop of refrigerant R-134a in a plate heat exchanger," Int. J. Heat Mass Transf., **42**(6), pp. 993–1006.

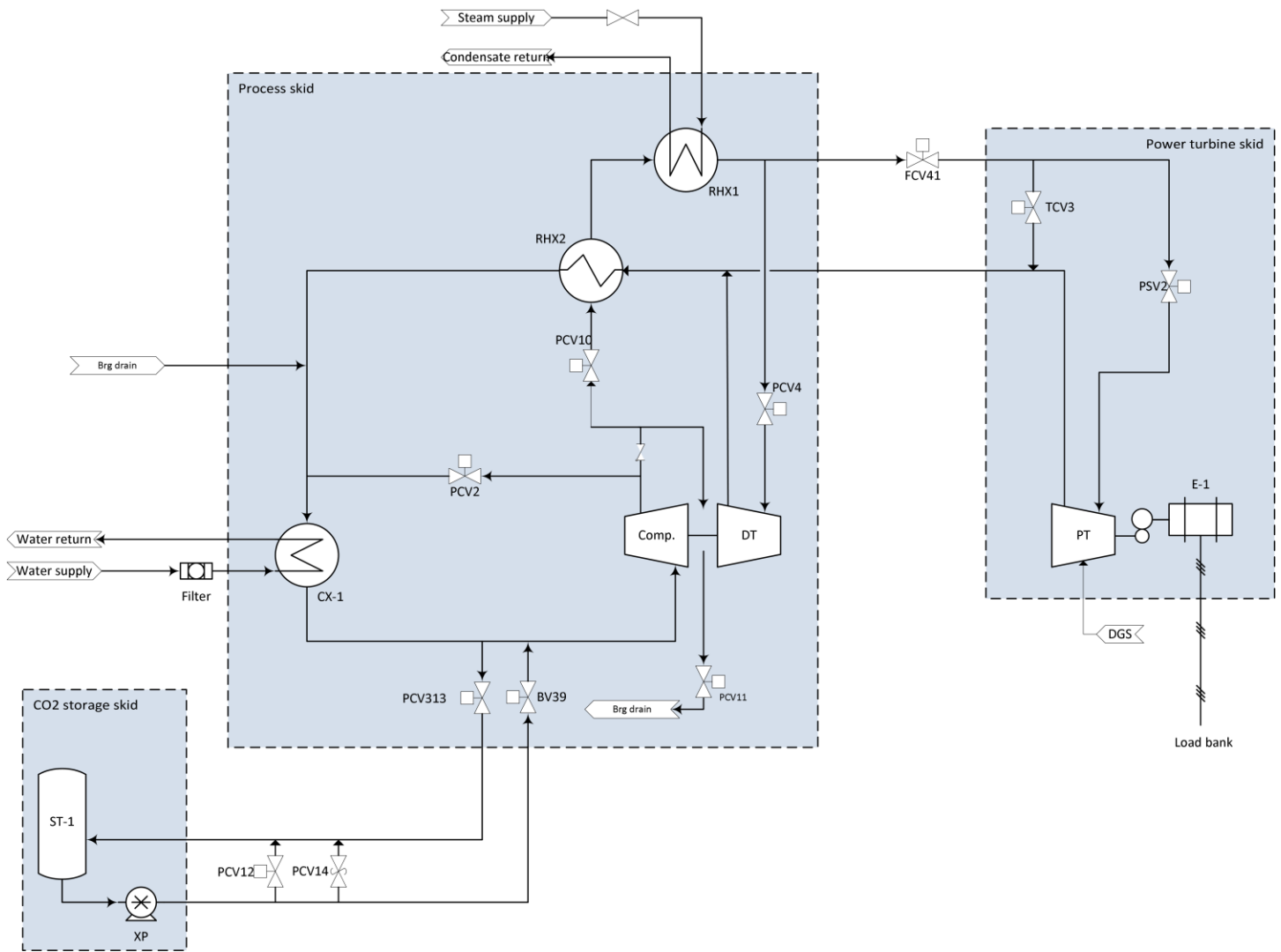


Figure 1: sCO₂ power cycle test configuration

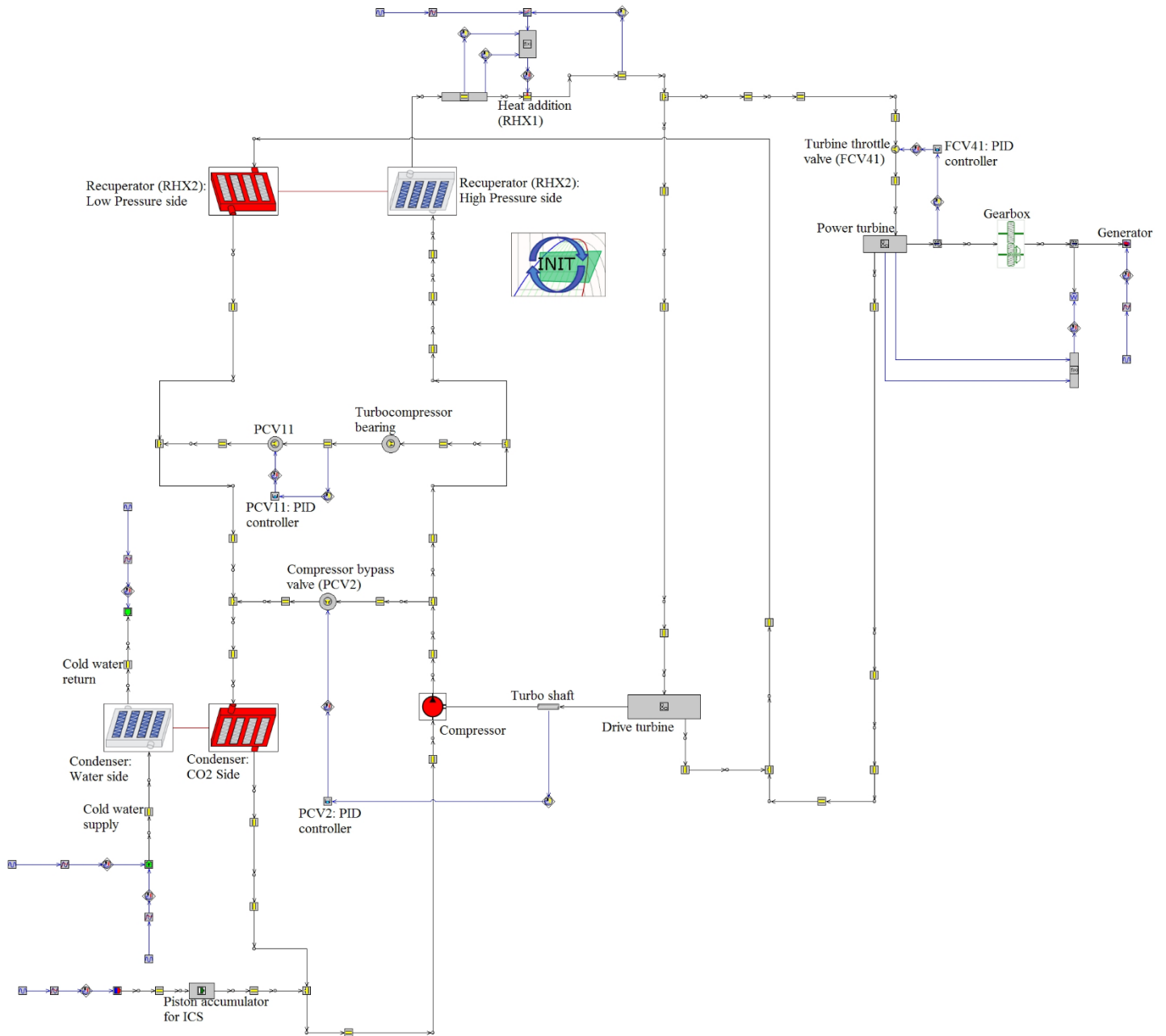


Figure 2: sCO₂ power cycle model configuration.

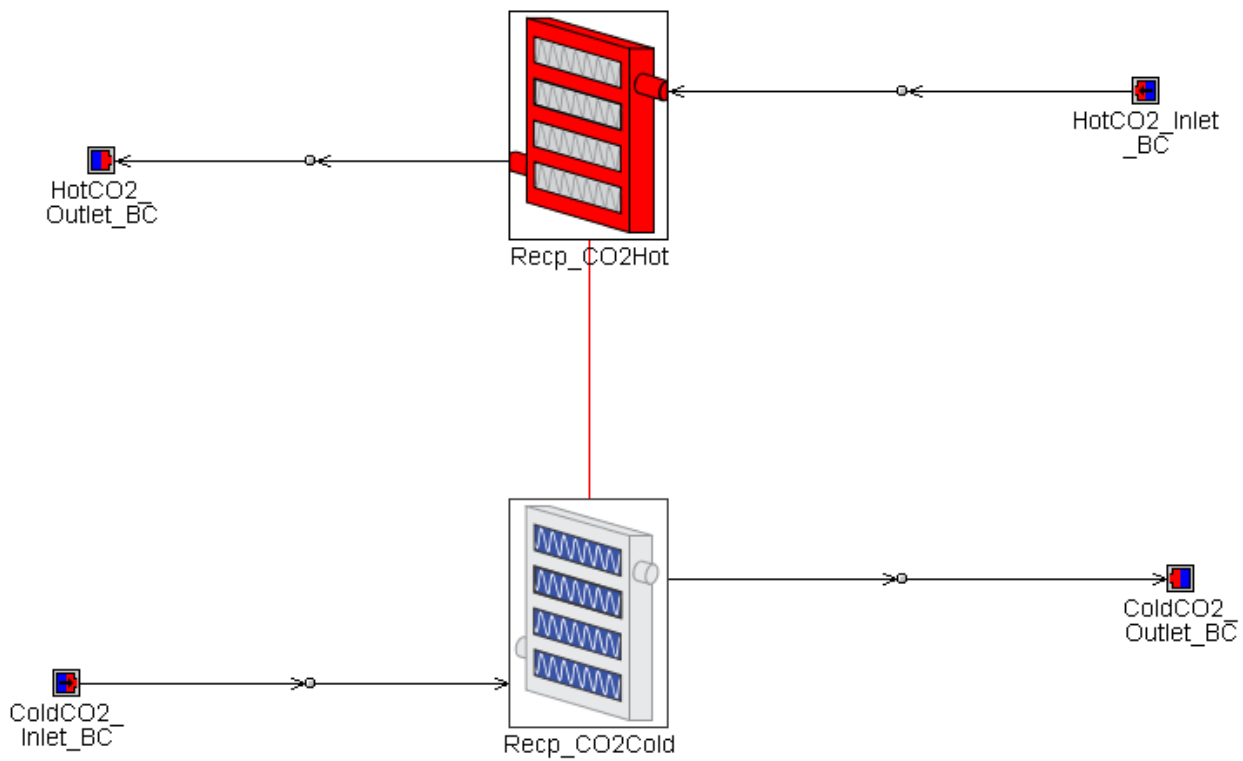


Figure 3: Recuperator component model with boundary conditions for calibration.

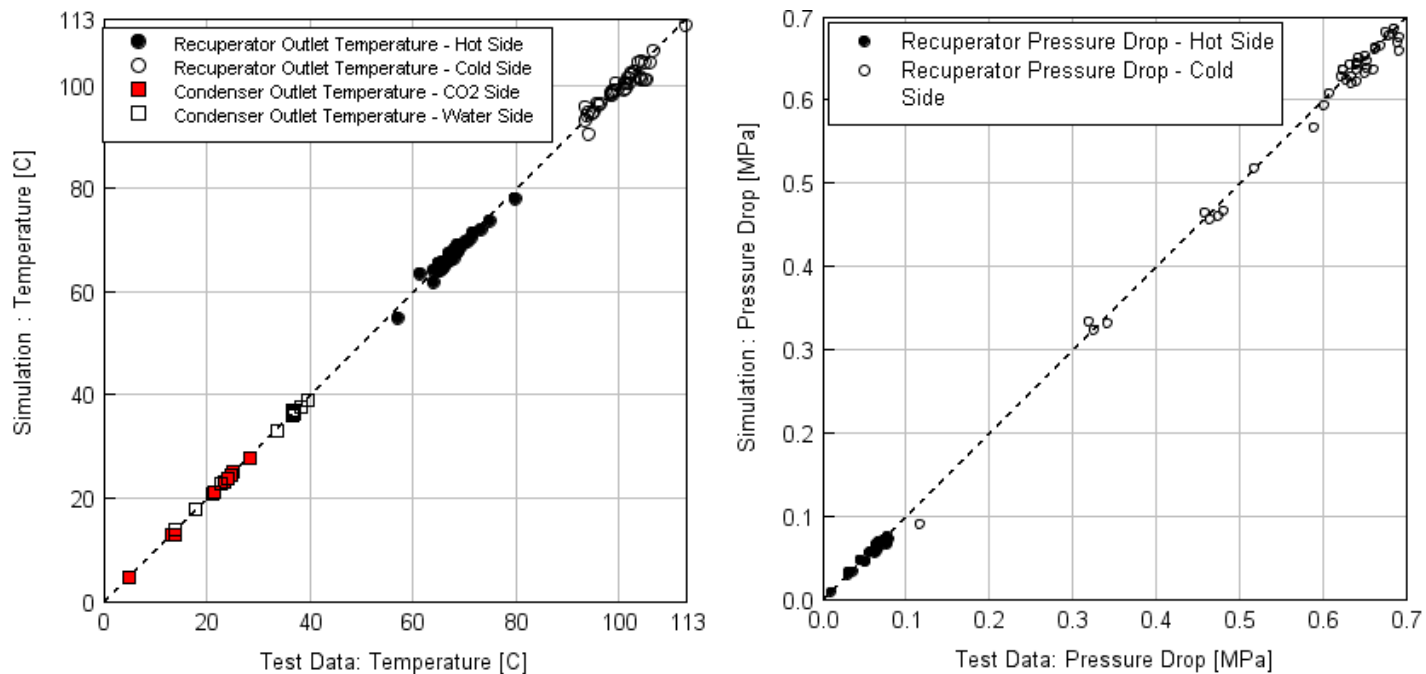


Figure 4: Recuperator and HRHX validation calculations.

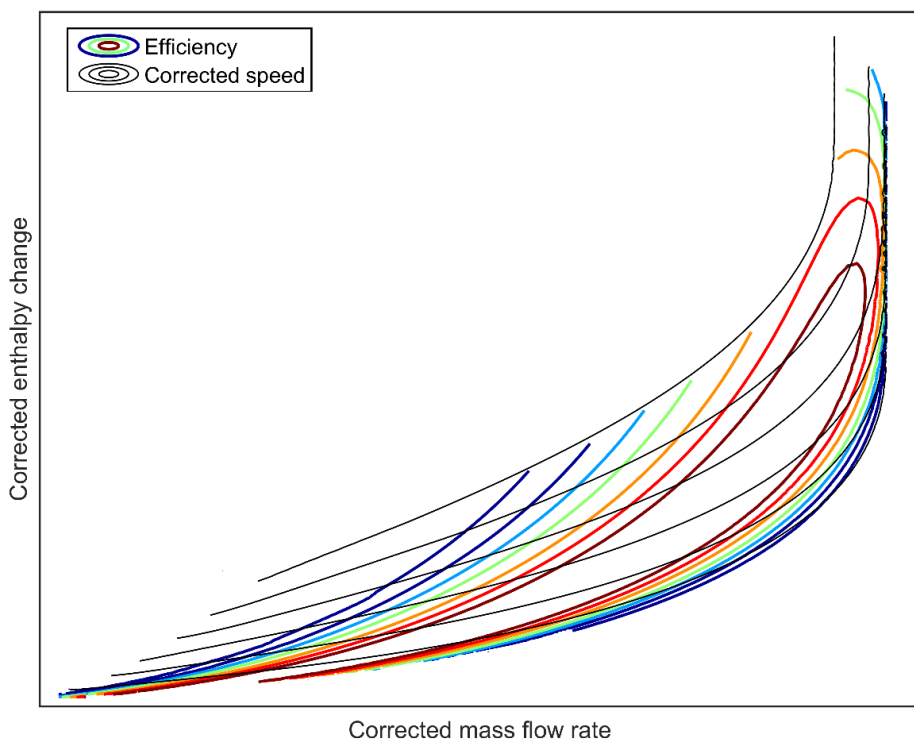


Figure 5: Sample turbine map. Color contours are constant isentropic efficiency, black contours are corrected speed.

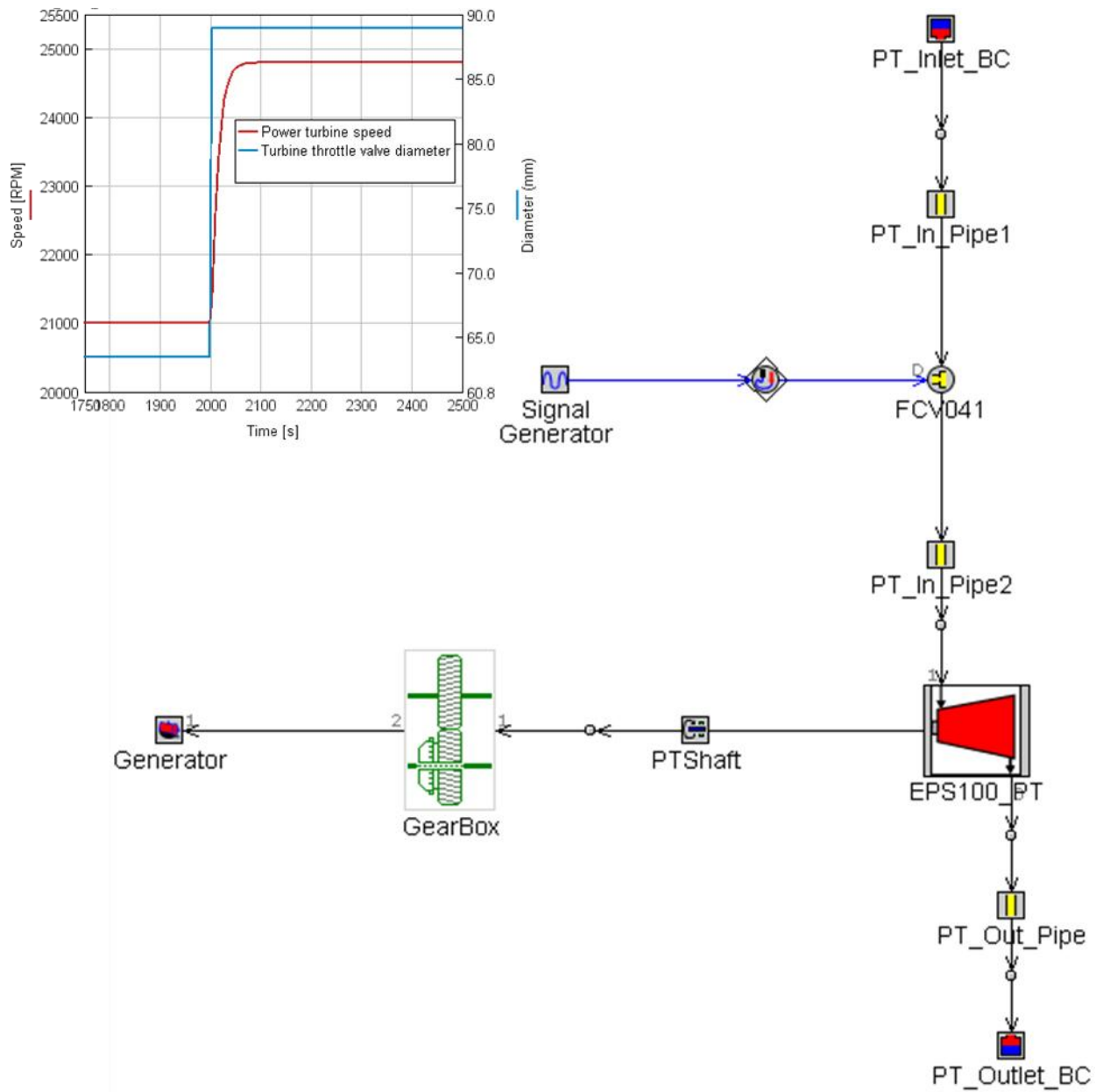


Figure 6: Power turbine throttle valve control loop step function

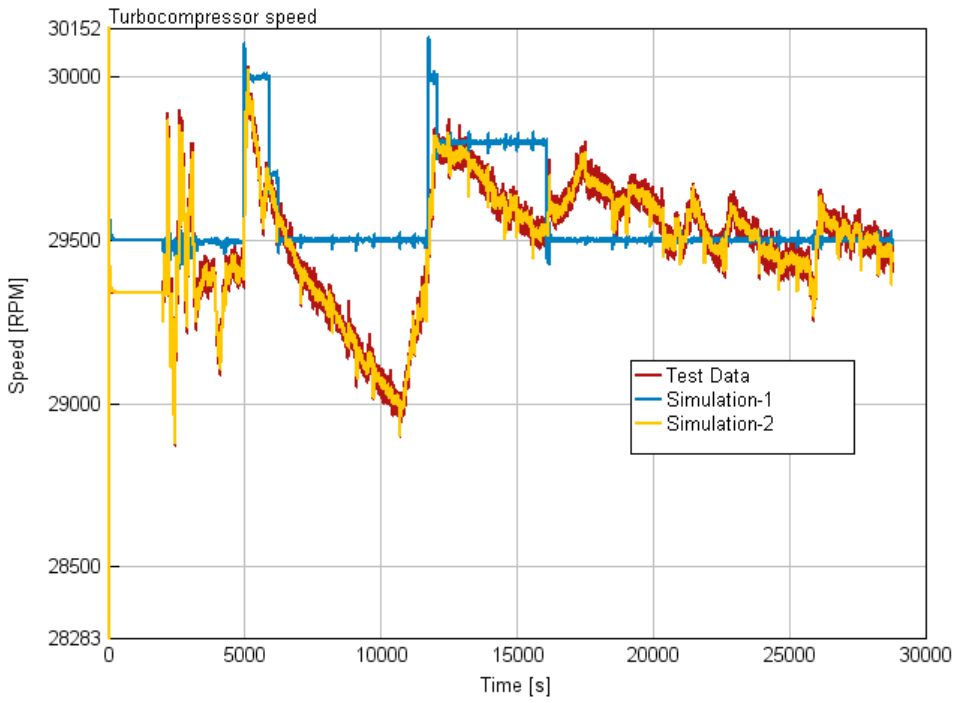


Figure 7: Turbocompressor speed

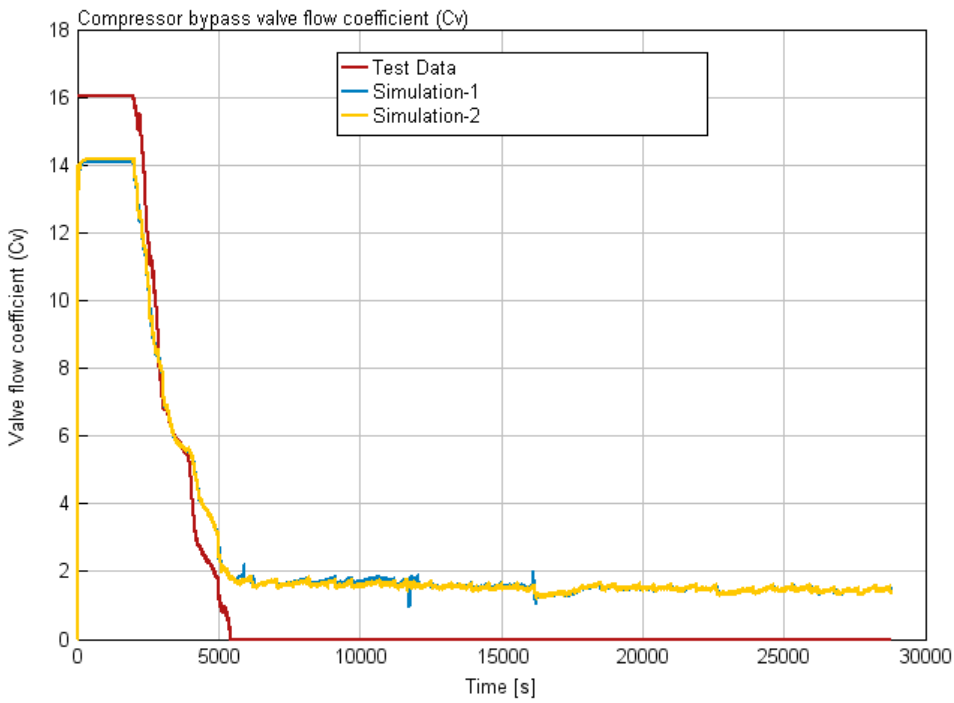


Figure 8: Compressor bypass valve flow coefficient

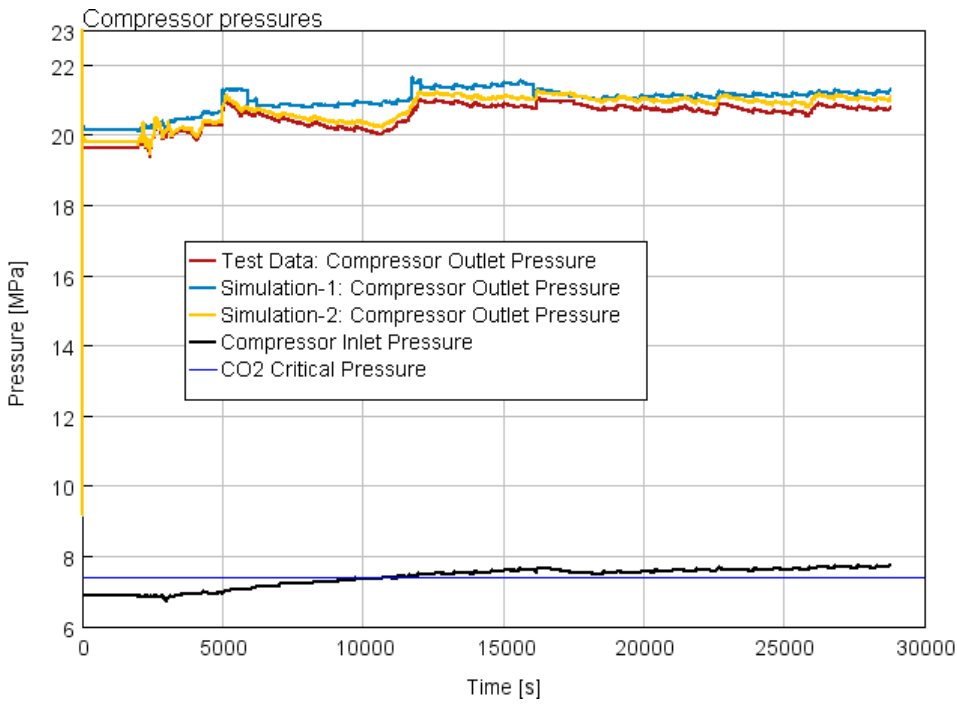


Figure 9: Compressor inlet and outlet pressures

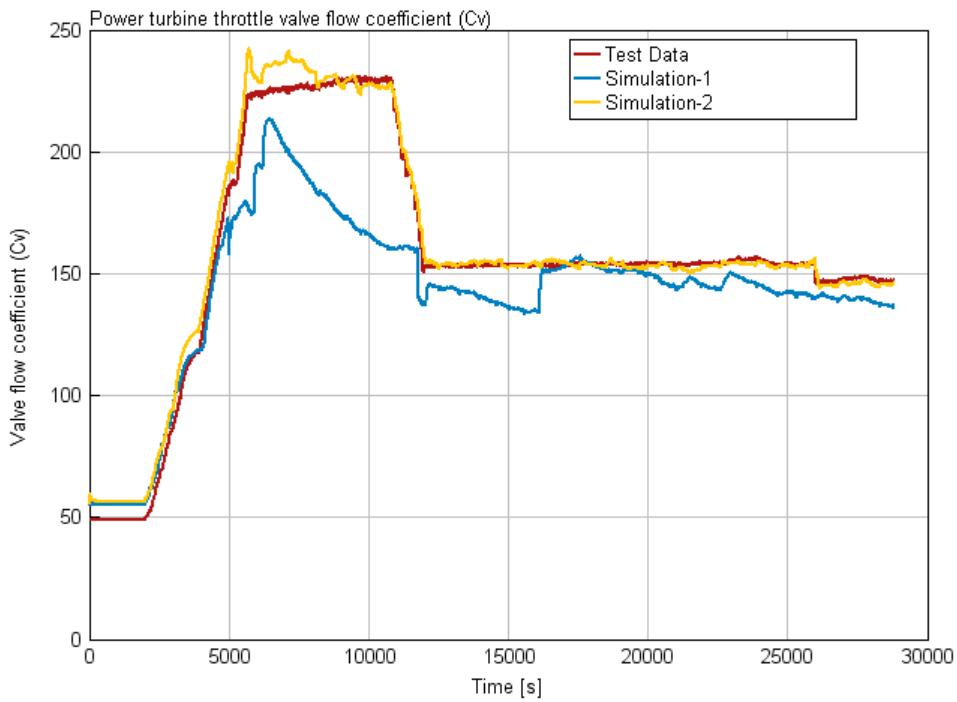


Figure 10: Power turbine throttle valve flow coefficient

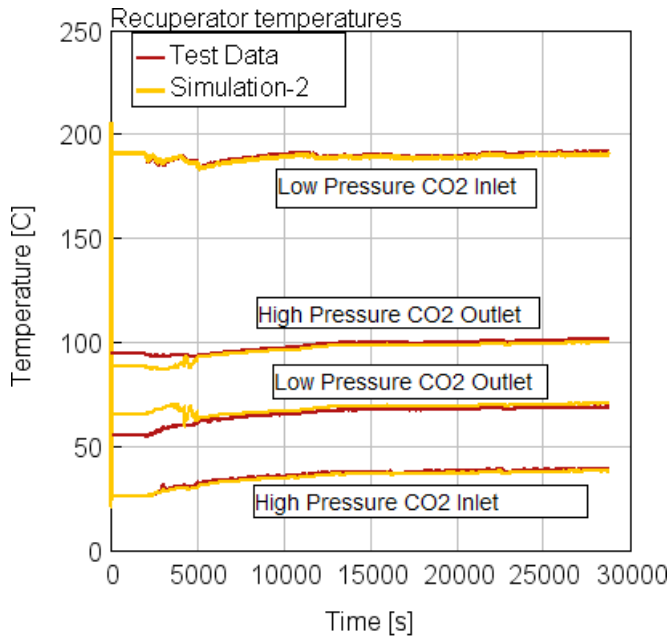


Figure 11: Recuperator inlet and outlet temperatures

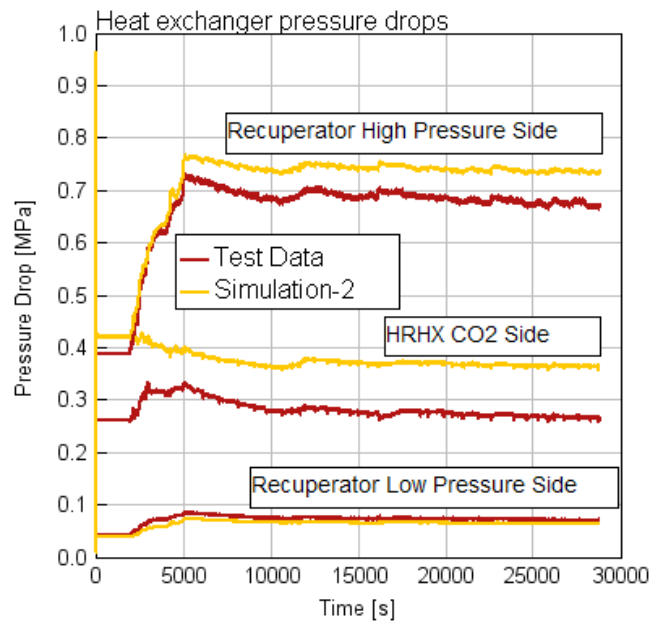


Figure 12: Heat exchanger pressure drops

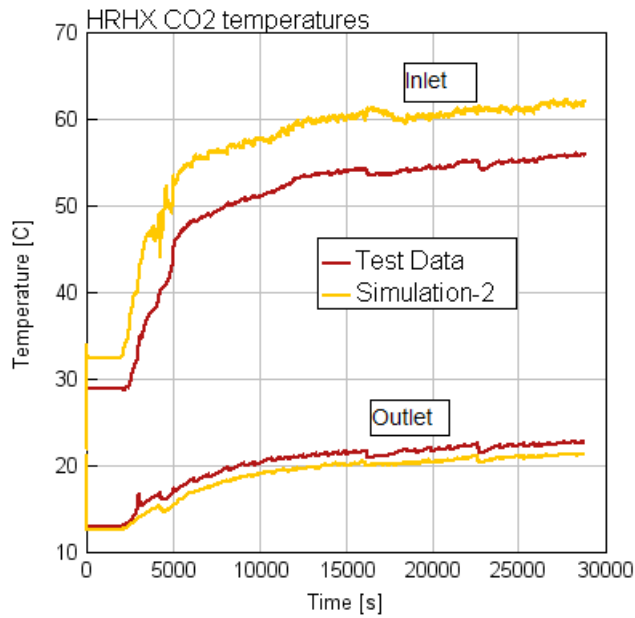
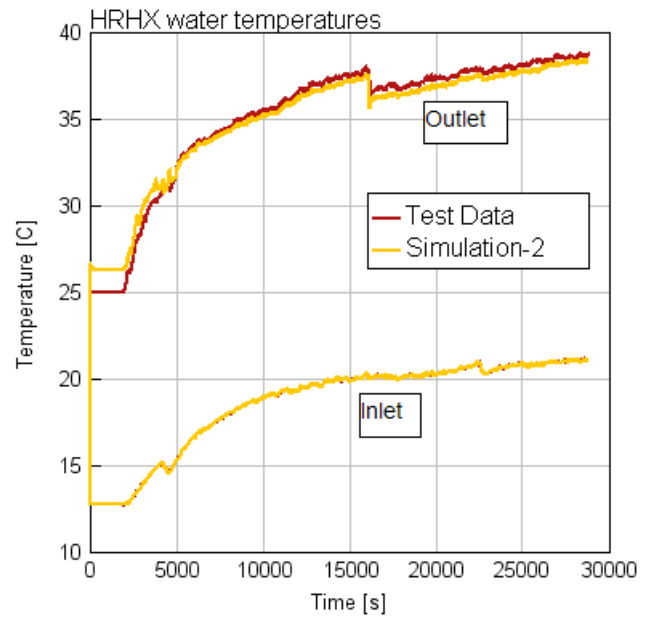


Figure 13: Heat rejection heat exchanger inlet and outlet temperatures



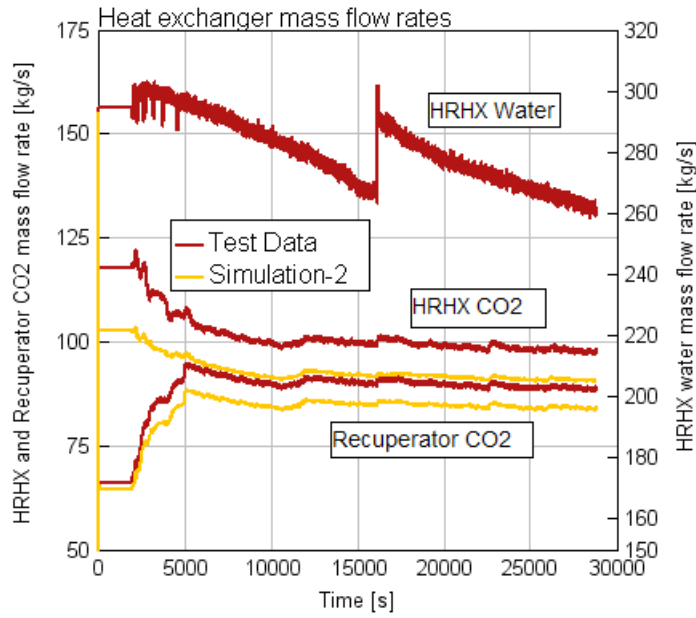


Figure 14: Heat exchanger mass flow rates

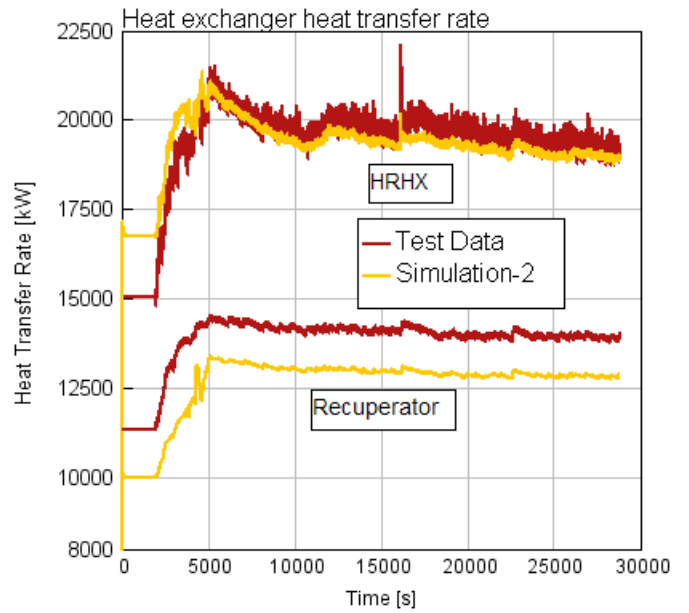


Figure 15: Heat exchanger heat fluxes

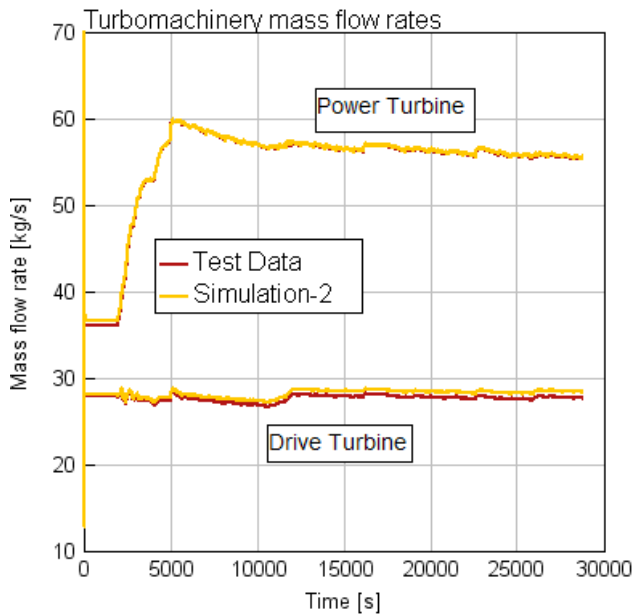


Figure 16: Turbomachinery flow rates

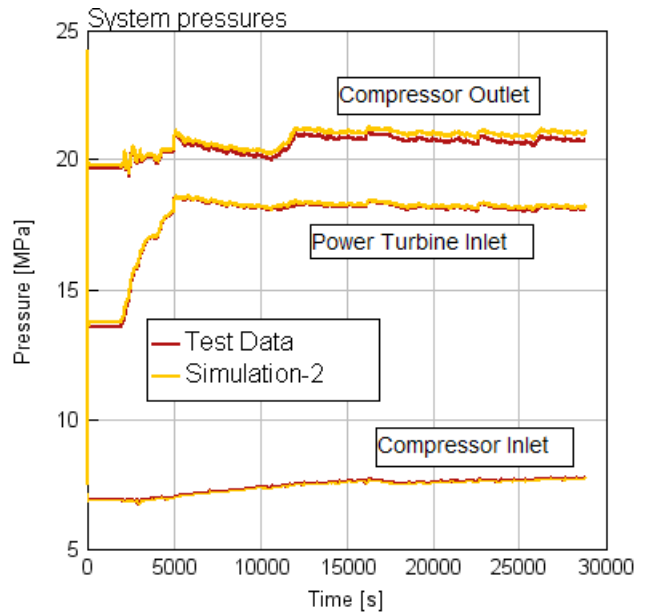


Figure 17: Turbomachinery inlet and outlet pressures

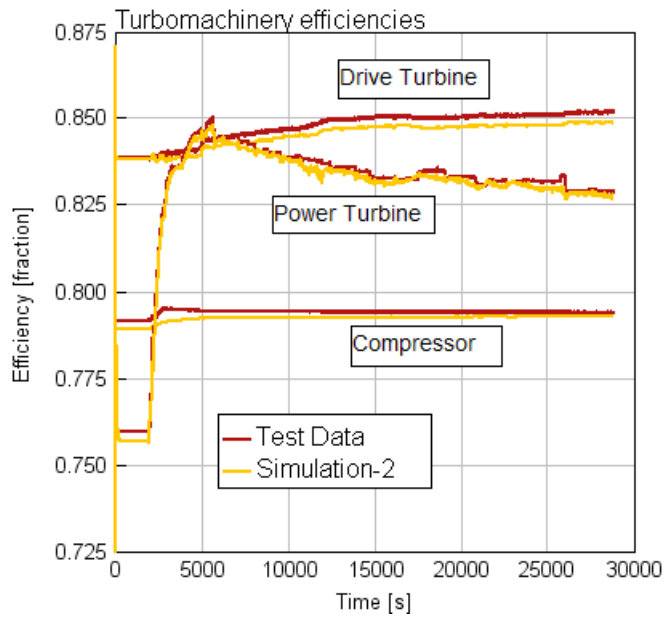


Figure 18: Turbomachinery efficiencies

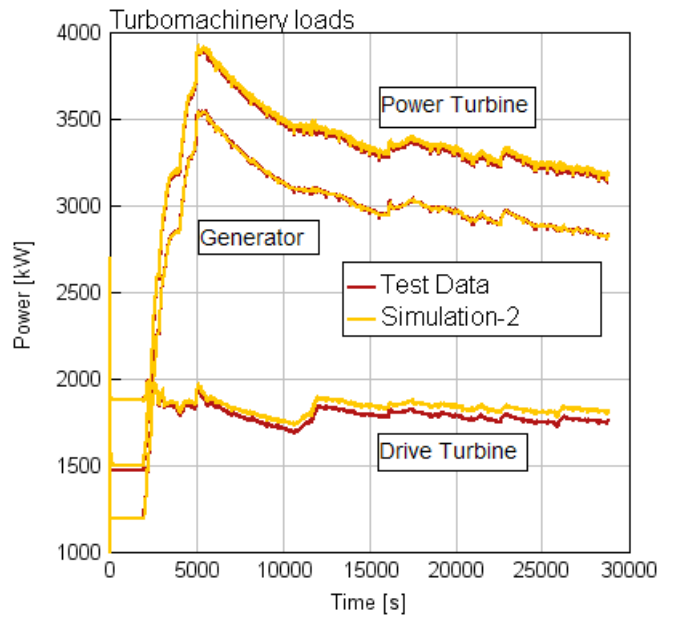


Figure 19: Turbomachinery work